Phys. Status Solidi C **11**, No. 9, 1452–1454 (2014) / **DOI** 10.1002/pssc.201300623

physica status solidi c
www.pss-c.com
current topics in solid state physics

Formation of ordered array of core/shell ZnS/Ge/ZnS nanostructures by thermal evaporation method

A. Beltiukov[*,1], R. Valeev[1,2], E. Romanov[2], and V. Mukhgalin[1]

[1] Physical-Technical Institute UB RAS, Izhevsk, Russia
[2] Udmurt State University, Izhevsk, Russia

Received 30 September 2013, revised 23 January 2014, accepted 26 March 2014
Published online 6 May 2014

Keywords semiconductor nanohetrostructures, porous anodic alumina, ZnS, Ge, high vacuum thermal deposition

* Corresponding author: e-mail beltukov.a.n@gmail.com, Phone: +7 3412 430163, Fax: +7 3412 722529

This paper reports the results of studies of ZnS/Ge/ZnS nanostructures, obtained by high vacuum thermal deposition of ZnS and Ge powders into porous anodic aluminium oxide (AAO) with different diameters of pores. Scanning electron microscopy (SEM) investigations reveal two types of nanostructures having the form of rings (sample with diameter of pores 70 nm) and rods (samples with diameter of pores 80 and 110 nm). It is also shown that the other porosity parameters such as interporous distances affect the formation of a particular type of nanostructures. X-ray and electron diffraction study show two phases, ZnS and Ge.

1 Introduction ZnS and Ge are widely used in optoelectronic devices as the materials of light emission and detection structures in blue and IR range of optical spectra respectively [1-3], and the achievements of last decades allowed to form different nanostructures based on them [4-7]. Particular interest is attracted to the layered structures, more of them are in the film form [8], but in [9] the core/shell Ge/ZnS hetero-nanowires were reported. There are also investigations of Ge/Si core/shell nanorods [10], ZnS/Si nanopillar arrays [11].

It is known that the optical and electronic properties of semiconductors are determined by their electronic structure and may by modified by creating multiform nanostructures. ZnS and Ge are wide gap and narrow gap semiconductors with the band gap energies of 3.56 eV and 0.67 eV, respectively. It is expected that the combination of properties of these materials can provide the improvement of luminescent and light absorption characteristics due to effects on ZnS/Ge and Ge/ZnS interfaces.

However most of the works have been devoted to systems where nanostructures have nonhomogeneous distribution in size and interparticle distances. Both these parameters have great importance on electronic and optical properties of composites. In the present study we focused on the synthesis and properties of ZnS/Ge structure arrays formed in porous anodic alumina oxide (AAO) matrix with quasiordered distribution of pores. It should be mentioned that the main aim of this work is technological testing of method of core/shell nanostructures formation. Due to this fact using of AAO matrices with quasiordered distribution of pores is enough.

ZnS/Ge nanostructures were synthesized by physical vapor deposition of ZnS into porous aluminum oxide templates. The microstructure and crystal structure were studied using scanning electron microscopy (SEM), X-Ray diffraction (XRD), Atomic force microscopy (AFM) and Transmission electron microscopy (TEM) with electron diffraction techniques.

2 Experimental

2.1 Sample preparation Matrices of porous alumina were prepared in a 0.3 molar solution of the oxalic acid at 0 °C and three different anodic voltages. As the result three samples with the different pore structure were obtained. The pore diameter and the wall thickness between pores were determined using an atomic force microscopy (Table 1).

A nanocomposite system consisting of the germanium core and the wide-gap shell of zinc sulphide was formed at three stages. At the first stage the surface of the porous

alumina at 200 °C was covered by a thermal evaporation of ZnS powder in high (10^{-5} Pa) vacuum [12]. The layer thickness was chosen so as to prevent complete filling and closing the pores. It was controlled by the AFM. Then the samples were covered by thermaly deposited Ge [13]. The pores were completely closed by germanium layer. Finally, the germanium layer was covered by the ZnS layer.

Table 1 Parameters of porous alumina matrices.

Sample	Solution	Anodic voltage, V	Diameter of pores, nm	Wall thickness, nm
1	0.3 M $C_2H_2O_4$	75	67 ± 5	37 ± 8
2		130	83 ± 8	76 ± 19
3		160	109 ± 18	139 ± 18

2.2 Investigation methods For SEM and AFM samples were fixed on a carbon tape and the matrix was selectively dissolved in 5 % H_3PO_4.

AFM images were obtained in contact mode by SolverPro (NT MDT) using standard silicon probe.

SEM investigations were carried out by Supra 50 VP instrument (LEO) equipped with energy-dispersive X-ray (EDX) analysis system Oxford INCA Energy+.

EDX analysis was performed to determine the distribution of material in the depth of pores. For this purpose the cross-section of the samples was studied.

TEM analysis was performed with microscope EM-125 (Ukraine) at 100 kV. For TEM investigations the part of the film with nanostructures was scraped from the carbon tape.

X-ray diffraction patterns were recorded in the 2θ range of 20–60° using a BRUKER D8 advance X-ray diffractometer with Cu-Kα radiation. Registration was carried out in grazing incidence angle mode using single Gobel mirror, incident angle – 1°. Si (Li) solid state detector is used for detection of X-ray radiation. XRD analysis was carried out on as-synthesized samples.

3 Results and discussion The samples were cleaved for EDX investigation of cross-section. Figure 1 illustrates the distribution of Ge, Zn and S in the depth of porous alumina. The distance was determined from the edge of the film to the bottom of pores.

Maximum concentration of elements is observed close to film/oxide interface marked in Fig. 1 by vertical line, and decreases rapidly with depth. It means that nanostructures can be formed only on the top of pores.

The concentrations of Zn and S in the first and second samples are close to stoichiometric. But inside the pores the sulfur concentration is greater than zinc concentration. This is probably due to the difference of the adhesion coefficient of zinc and sulfur to the pores walls. But in the third sample with the biggest size of pores diameter Zn and S concentrations are not stoichiometric.

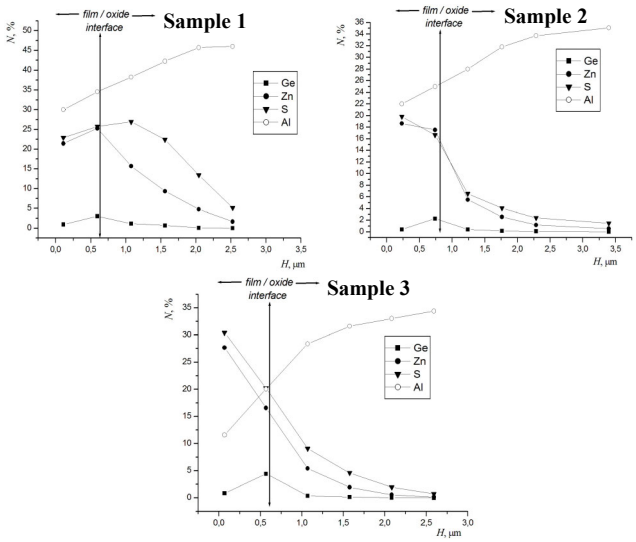

Figure 1 Distribution of Ge, Zn and S in the depth of porous alumina. Vertical line shows the film/oxide interface.

After removing the alumina matrices we have found the nanostructures on the surface of films by SEM (Fig. 2). In the first sample we have observed the tubular structure. The height is 54 nm, the outer diameter is 57 nm, and the inner diameter is 26 nanometers. In the second and third samples we have observed the rod structures. The height of the obtained rods in the second sample is 65 nm and their diameter is 83 nm. In the third sample the height of the rods is 131 nm and the diameter is 109 nm. The parameters of obtained nanostructures were investigated by AFM.

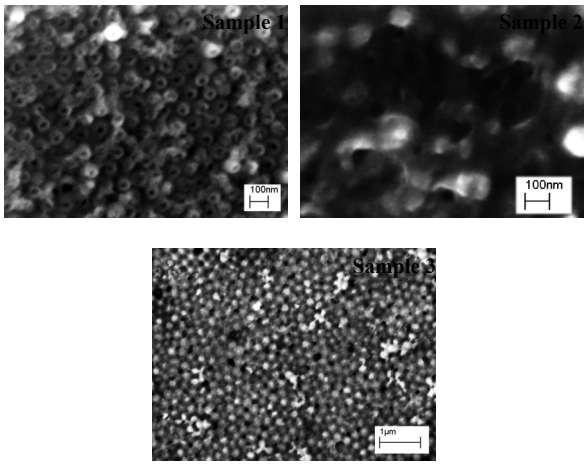

Figure 2 SEM images of ZnS/Ge/ZnS nanostructures grown by thermal evaporation of material in high vacuum on the porous alumina substrates.

It is also seen from Fig. 2 that the nanostructures replicate the location and size of the pores of alumina matrix. The height of the nanostructures depends on the filling depth of the pores. Filling the pores at thermal evaporation and forming the nanostructure are observed in two direc-

tions. If the wall thickness between pores is less than their diameter (the first sample, for example) the film growth on the alumina surface between pores leads to the pores sealing on top. There is no time enough to close pores completely and therefore the tube structure is formed. If the wall thickness between pores is greater than their diameter, filling the pore is observed from the wall to its center. In this case the pores are filled completely forming a rod structure.

X-ray diffraction (Fig. 3) shows 2 phases, ZnS and Ge. As for ZnS three diffraction maxima are observed, (111), (220) and (311). For Ge we have observed only one maximum (111). The absence of reflection from a plane (200) shows the texture. It means that the crystals are oriented along the growth direction (111).

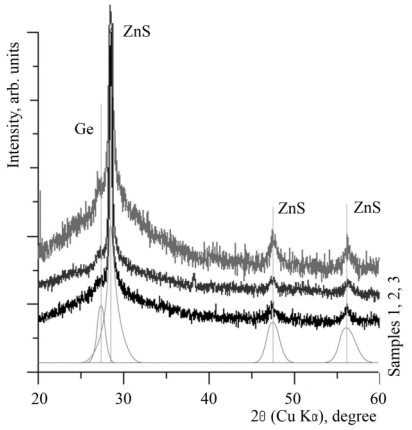

Figure 3 XRD patterns of ZnS/Ge/ZnS nanostructures in AAO films. ZnS in cubic (JCPDS # 01-071-5975) phase and Ge in cubic (JCPDS # 00-0040545) phase.

Electron diffraction (Fig. 4) confirms the presence of texture. As can be seen the nanostructures located in the honeycomb consist of smaller blocks. Size distribution of these blocks is in the range from 10 to 30 nm. The rings of the diffraction pattern also show the polycrystalline structure.

The lattice constant has been calculated from the electron diffraction pattern. For ZnS the lattice constant is 5.41 ± 0.02 Å and close to crystallographic value (5.4195 Å). But for germanium the lattice constant is smaller than the theoretical value (5.59 ± 0.05 Å as compared with crystallographic value 5.6576 Å). Probably the shell of ZnS compresses the crystallites of Ge and therefore the lattice constant of Ge decreases.

4 Conclusion ZnS/Ge/ZnS core/shell rods and rings were synthesized by thermal evaporation of ZnS and Ge powder on porous surface of anodic alumina oxide. Deposition into AAO with diameters of pores 70 nm results in formation of rings-like nanostructure whereas deposition into AAO with diameters of pores 80 and 110 nm results in formation of rod-like structures. X-ray and electron diffraction studies show the presence of ZnS and Ge phases. The lattice constant of ZnS is close to crystallographic value. The germanium crystallites have a compressive stress and therefore the lattice constant of Ge decreases.

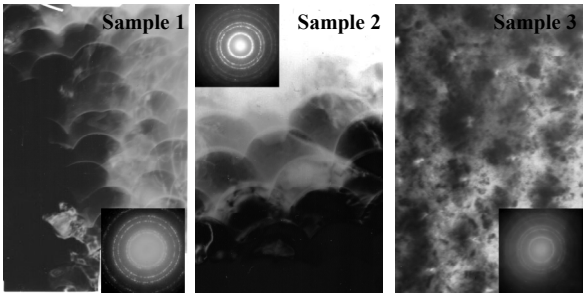

Figure 4 TEM images of ZnS/Ge/ZnS nanostructures. Magnification of samples is 150,000 x.

Acknowledgements The authors are grateful to Ilya Roslyakov (Materials Science Department of Lomonosov's Moscow State University) for SEM and EDX study and Nikolay Kostenkov (Udmurt State University) for TEM and electron diffraction images. This work is supported by UB of RAS projects No. 12-P-2-1038 and 12-S-2-1024.

References

[1] S. H. Deulkar, C. H. Bhosale, and M. Sharon, J. Phys. Chem. Solids **65**, 1879 (2004).
[2] J. Vidal, O. De Melo, O. Vigil, N. Lopez, G. Contreras-Puente, and O. Zelaya-Angel, Thin Solid Films **419**, 118 (2002).
[3] G. Masini, V. Cencelli, L. Colace, F. DeNotaristefani, and G. Assanto, Physica E **16**, 614 (2003).
[4] O.P. Pchelyakov, A.I. Nikiforov, B.Z. Olshanetsky, S.A. Teys, A.I. Yakimov, and S.I. Chikichev, J. Phys. Chem. Solids **69**, 669 (2008).
[5] J. Lee, K.L. Wang, H.-T. Chen, and L.-J. Chen, J. Cryst. Growth **301–302**, 330 (2007).
[6] X. Liu, J. Cui, L. Zhang, W. Yu, F. Guo, and Y. Qian, Mater. Lett. **60**, 2465 (2006).
[7] N. Taghavinia and T. Yao, Physica E **21**, 96 (2004).
[8] G. É. Frank-Kamenetskaya, K. K. Murav'eva, and I. P. Kalinkin, Sov. Phys. J. **21**, 925 (1978).
[9] G. Z. Shen, D. Chen, and C. Zhou, Chem. Mater. **20**, 3788 (2008).
[10] J. Xiang, W. Lu, Y. Hu, Y. Wu, H. Yan, and C.M. Lieber, Nature **441**, 489 (2006).
[11] H.J. Xu and X.J. Li, Semicond. Sci. Technol. **24**, 075008 (2009).
[12] R. Valeev, E. Romanov, A. Beltukov, V. Mukhgalin, I. Roslyakov, and A. Eliseev, Phys. Status Solidi C **9**, 1462 (2012).
[13] R.G. Valeev, D.V. Surnin, A.N. Beltyukov, V.M. Vetoshkin, V.V. Kriventsov, Ya.V. Zubavichus, N.A. Mezentsev, and A.A. Eliseev, J. Struct. Chem. **51**, S132 (2010).

